Hydrothermal stability of water sorption ionogels

Hydrothermal stability of water sorption ionogels

Hongsheng Dong[1,4], Ahmed A. Askalany[2,3], Christopher Olkis[2], Jiafei Zhao[4*], Giulio Santori[2*]

[1] Dalian Institute of Chemical Physics, Chinese Academy of Sciences, Dalian 116023, China

[2] The University of Edinburgh, Institute for Materials and Processes, EH9 3BF Edinburgh, UK

[3] Mechanical Engineering Department, Faculty of Industrial Education, Sohag University, Sohag, 82524, Egypt

[4] School of Energy & Power Engineering, Dalian University of Technology, Dalian 116024, China

[*]Corresponding author: jfzhao@dlut.edu.cn, G.Santori@ed.ac.uk

Abstract

Adsorption desalination and membrane distillation are the only thermally driven desalination technologies that can be undertaken at temperatures below 70°C. Adsorption desalination is based on an adsorber whose performance primarily depends on the properties of the water sorbent. Water sorption ionogel represents a novel class of materials offering a large working capacity for desalination. In this study, water-sorptive ionogels were prepared and their hydrothermal stability was assessed. The results show that Syloid 72FP silica-based ionogels are hydrothermally stable. The ionic liquid EMIM Ac can be tightly confined in silica at amounts of up to 50 wt% and still withstand high relative humidity and temperature swings. Water uptake of the synthesized ionogel can be up to 1.64 g_{water} $g_{ionogel}^{-1}$ at 90% RH, which is ~3 times of that of Syloid 72FP silica and ~4 times of that of activated carbon. The EMIM Ac/Syloid 72FP ionogel thus exhibits features appropriate for adsorption desalination systems.

Keywords: Ionic liquid; Silica; Ionogel; Adsorption desalination.

1. Introduction

Ionic liquids (ILs) are salts with a melting point below 100°C [1]. The physicochemical properties of ILs can be finely tuned by a suitable choice of cation and anion. As a result, these solvents can be designed for a particular application or to present a particular set of intrinsic properties [2, 3]. Because of this advantage, ILs are used in catalytic reactions as solvents [4], separation [5], in fuel cells as electrolytes [6] and as heat transfer fluids [7] as well as in biotechnological and engineering processes [8]. For instance, Bates et al. reported a novel IL that can readily and reversibly sequester CO_2 [9]. Heym et al. used ionic liquids to dry gases by absorption[10]. Aken et al. expanded the operating potential window of electrochemical capacitors based on the formulation of appropriate IL electrolytes [11]. Askalany et al. prepared silica supported IL composite material for high throughput desalination and drying [12].

Desalination offers a solution to supplement the natural freshwater resources [13, 14]. Adsorption desalination (AD) is an emerging thermally driven method that is proven to be energy efficient and environmentally friendly [15, 16]. Figure 1 shows a schematic diagram of a two-bed adsorption desalination system. This system consists of four major components: a condenser, two sorption beds, and an evaporator [17, 18]. Under two-bed operation mode, one

sorption bed adsorbs while the second bed desorbs [19]. This allows the system to desalinate continuously. The basic working principle of an AD cycle consists of water vapor sorption by an unsaturated sorbent in one half-cycle period [20, 21] and sorbent regeneration in the next half-cycle by heating it with a low temperature heat source in the range of 40–85°C [22, 23]. Regenerated vapors from the desorber are condensed on the surfaces of the condenser and are collected as potable water [24]. It is well known that the performance of the AD cycle depends on the adsorbents [25, 26]. A considerable number of studies have been conducted on adsorbents such as silica gel and zeolite [16, 17, 27-29]. Unfortunately, the regenerating temperatures are usually >60°C [30, 31] which are not always available. Therefore, it is desirable to find alternative adsorbents which can efficiently process large amounts of water with low regenerating temperatures [32].

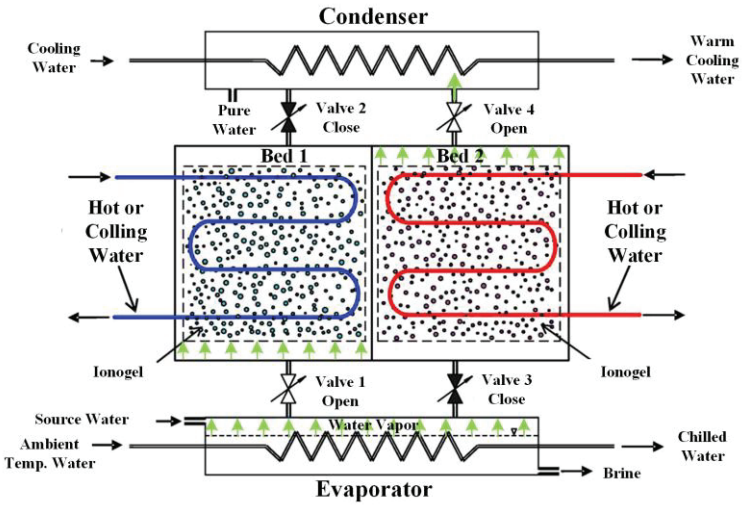

Figure 1. Schematic representation of an adosprtion desalination system [33].

Most ILs, due to their ionic character, readily absorb water from the environment [34, 35]: even hydrophobic ILs absorb traces of water very rapidly [36]. This interesting property can be beneficial for use in AD. Except high hygroscopicity, ILs for adsorption desalination should also have other unique properties, i.e., they should have negligible vapor pressure, be nonflammable, show thermal and chemical stability in air and water, and be recyclable when applied in AD [37]. One of the drawbacks of ILs is, however, that they are liquid, which limits their application in many devices [38]. For real applications, ILs are even more useful if immobilized in a solid porous matrix as a means to overcome leakage problems [39]. The immobilization of ILs within organic or inorganic matrices results in composite materials called ionogels [40, 41]. To immobilize an IL in a solid support, choice of the support type and immobilization method is important. As for the support, silica nanoparticles have been used in recent years as supports for the immobilization of ILs in order to improve their applicability and reusability [42], because they are among the most popular porous materials and exhibit a combination of excellent adsorption characteristics and high particle stability [4]. As for the immobilization method, chemical immobilization is often preferred for volatile compounds because it prevents loss of the immobilized species, but it often incurs a high cost. However, in immobilizing an IL for gas–solid applications, a relatively weak physical

interaction between support and the IL may be adequate owing the very low volatility of the IL [43]. A number of ionogels have been prepared using silica and physical immobilization [39, 42, 44, 45], and their features such as ionic transport and viscoelastic properties have been studied [46, 47]. Ionogels incorporating highly hygroscopic ILs can be potentially used as adsorbents for AD but there have been few studies on the hydrothermal stability and adsorption behavior of ionogels.

Thus, the purpose of this investigation is to synthesize ionogels with excellent stability and adsorption behavior. We synthesized a series of ionogels using silica nanoparticles and EMIM Ac by incipient wetness impregnation. The IL confinement of ionogels was verified to achieve high IL loading and free-standing ionogels. The hydrothermal stability was examined at two RH levels. Finally, the adsorption behavior was analyzed to clarify the feasibility of using the ionogel for AD.

2. Materials and method

Syloid FP silicas are micronized synthetic amorphous silica gels of high purity. They have a highly developed network of mesopores that provide access to their large surface area. The unique combination of their adsorptive capacity, mesoporosity, particle size, and surface morphology allow them to be used as supports for ionogels. During the compression cycle of the tableting process, liquid ingredients can be forced to the surface or even be forced to exude from the tablet. However, Syloid FP silica provides greater IL retention and prevents the occurrence of the above problem. The properties of two Syloid FP silica nanoparticles used in the study are compared in Table 1.

Table 1. Comparison of Syloid AL-1FP and 72FP.

Property	Syloid AL-1FP	Syloid 72FP
SiO_2 (dried basis) (%)	99.6	99.6
Average particle size (μm)	7.5	6.0
Oil adsorption (l g/100 g)	80	220
Bulk density (g/L)	566	112
Average pore volume (mL/g)	0.4	1.2

The vapor–liquid equilibria of various ILs were reviewed and six typical ILs were selected to compare their water uptake, as shown in Figure 2. Compared with other ILs, EMIM Ac shows higher hygroscopicity throughout the entire RH range tested. Table 2 shows that EMIM Ac has low vapor pressure, high thermal stability, and non-flammability. Thus, EMIM Ac was selected for preparation of the ionogel in this study.

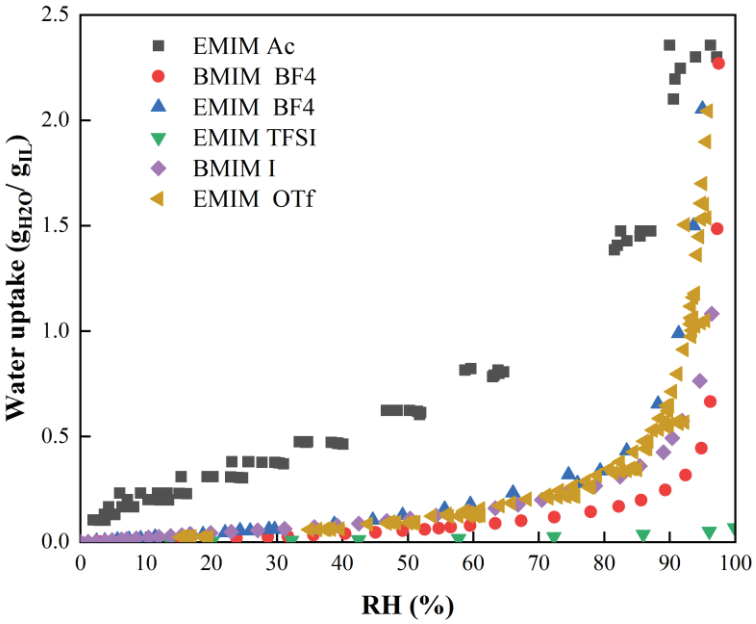

Figure 2. Comparison of water sorption capacity of different ILs [48-52].

Table 2. Thermophysical properties of EMIM Ac at 20°C.

Property	Value
Density[53]	1.1049 g/cm^3
Viscosity[54]	91 mPa·s
Thermal conductivity[53]	0.221 (W/m·K)
Specific heat capacity[53]	1.8560 kJ/(kg·K)
Flash Point	164°C
Pyrolysis temperature[2]	221°C
Melting point[54]	-45°C
Fire point[55]	nonflammable

A simple and inexpensive physical immobilization method, incipient wetness impregnation[56], was used in this study. Figure 3 schematically illustrates the process. The silica particles and IL were dried for 24 h in a vacuum oven at 80°C before use. EMIM Ac and a volatile solvent—deionized water—were mixed in a vial, and then the solid support (Syloid silica) and functional material (a binder in this case) were added into the vial. The impregnation was completed by mechanical mixing until homogeneity was achieved. The obtained samples were heated at 80°C to evaporate the volatile solvent (i.e., water) until there was no change in the mass. Then, the samples were sealed in glass vials. The obtained samples were again dried for 24 h under vacuum and heating at 80°C prior to use for each measurement. All ionogels were prepared under ambient laboratory conditions. A handheld ionogel-preparation device was used to press the ionogel powder into regular ionogels. The diameter and height of the ionogel sample were 6 mm and 2.5–4 mm, respectively.

IL confinement was visually inspected after the ionogel had been prepared freshly. To verify the hydrothermal stability of the ionogel, cyclic adsorption–desorption tests were carried out at room temperature. These tests were conducted at two RH levels. One cycle includes

adsorption and desorption. The adsorption time was 12 h at 60% RH while the adsorption time at 80% RH was 5 h. The samples were dried at 80 °C for desorption. The mass and morphology after adsorption and desorption were recorded at a regular interval.

Dynamic vapor sorption (DVS) is a well-established method for the determination of vapor sorption isotherms[57]. Adsorption equilibrium at 25 °C was recorded using a DVS automated gravimetric sorption analyzer (Surface Measurement Systems Ltd., London, UK). The instrument has a working humidity range of 0–98% RH with a sensitivity of 0.1 μg. The relative concentration around the sample was controlled by mixing saturated and dry carrier gas (N_2 in this case) streams using mass flow controllers. Prior to being exposed to any vapor, the samples were equilibrated for 6 h at 0% RH to remove any surface water present and establish a dry baseline mass. At each RH, the sample mass was allowed to reach equilibrium before the partial pressure was increased.

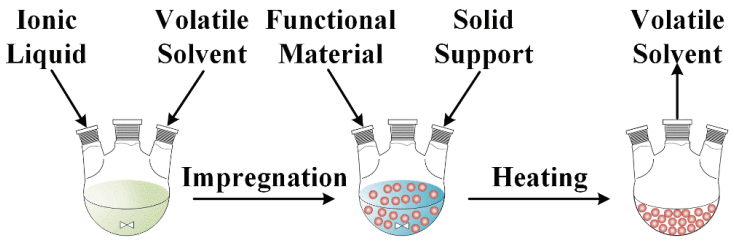

Figure 3. Procedure for preparing the ionogel.

Specifications of materials and devices used in the study are summarized in Table 3.

Table 3. Specifications of experimental materials and devices.

Name	Supplier	Purity/Precision
Syloid AL-1FP	Grace	99.6%
Syloid 72FP	Grace	99.6%
EMIM Ac	Sigma Aldrich	95.0%
Deionized water	Self-produce	
Balance	Sartorius, ED224S	0.1 mg
Oven	Thermo Fisher Scientific, Heraeus vacutherm	0.1°C
DVS automated gravimetric sorption analyzer	Surface Measurement Systems	

3. Results and discussion

3.1. IL confinement stability

Six ionogels with different EMIM Ac/silica mass ratios were prepared to examine the IL confinement stability. Table 4 compares the IL confinement stabilities of ionogels with different formulations at 60% RH. After EMIM Ac immobilization, the silica particles maintained a white color. Further addition of silica increased the hardness of the ionogels. The ionogels changed from transparent and white to opaque white with increasing amounts of

silica. For Syloid AL-1FP, when the proportion of EMIM Ac increased to 55 wt.%, the ionogel 45/55 Syloid AL1-FP/EMIM Ac was very soft and could not be self-standing; When the proportion of EMIM Ac decreased to 50 wt.% and 45 wt.%, the ionogels were compliant and maintained their original shape. Therefore, it can be inferred that the loading maximum of EMIM Ac in Syloid AL-1FP-based ionogel with good confinement was about 50 wt.% when the ionogel was freshly synthesized. For Syloid 72FP, as the IL proportion of ionogel decreased from 70 wt.% to 50 wt.%, the color of ionogel changed from light white to bright white. When the ionogels had been freshly prepared, all ionogels showed good IL confinement. It was observed that the mixture of 80 wt.% EMIM ac and 20 wt.% Syloid 72FP was a white slurry. Therefore, the maximum loading of EMIM Ac in Syloid 72FP can be considered to be about 70 wt.% when the ionogel is freshly prepared. It can be concluded that stable ionogels under ambient conditions can be obtained by five formulations out of the six tested, with the exception of 45/55 Syloid AL-1FP/EMIM Ac.

Table 4. Comparison of IL confinement stability of ionogels with different formulations at 60% RH.

ID	Formulation	Initial photo	Exposed in 60% RH air for 12 h
1	45 wt.% Syloid AL-1FP, 55 wt.% EMIM Ac		
2	50 wt.% Syloid AL-1FP, 50 wt.% EMIM Ac		
3	55 wt.% Syloid AL-1FP, 45 wt.% EMIM Ac		
4	30 wt.% Syloid 72FP, 70 wt.% EMIM Ac		
5	40 wt.% Syloid 72FP, 60 wt.% EMIM Ac		
6	50 wt.% Syloid 72FP, 50 wt.% EMIM Ac		

To further examine the stability of the ionogel, five other ionogels were exposed in air for 12 h. Obviously, the ionogel color for the 30/70 Syloid 72FP/EMIM Ac changed from opaque white to transparent white, the surface of this ionogel appeared moisturized with a small

amount of IL leakage, suggesting poor IL confinement. Ionogels 2, 3, 5, and 6 (in Table 4) showed good confinement stability at 60% RH. Therefore, when the proportion of silica nanoparticles was higher, the IL confinement was better. This is because the pore volume and surface area increase with increase in the amount of silica nanoparticles, which provides sufficient binding between the silica nanoparticles and the IL. In addition, Syloid 72FP can confine more IL in the ionogel than Syloid AL-1FP. This is due to the larger pore volume of Syloid 72FP compared to that of Syloid AL-1FP. Therefore, the ionogels 50/50 of Syloid AL-1FP/ EMIM Ac and 40/60 Syloid 72FP/EMIM Ac can be used to obtain with good IL confinement at 60% RH.

Nevertheless, in order to obtain high adsorption performance, more IL is required in the silica network. According to this requirement, the ionogels 50/50 of Syloid AL-1FP/ EMIM Ac and 40/60 Syloid 72FP/EMIM Ac were considered suitable. When an ionogel is used in AD, it is usually exposed to RH values of >70%. Thus, it is necessary to check the confinement stability in high-RH environments. As shown in Table 5, after exposure to 80% RH for 5 h, a large amount of liquid formed around the ionogels 50/50 of Syloid AL-1FP/ EMIM Ac and 40/60 Syloid 72FP/EMIM Ac. To verify if the liquid on the surface was condensed water or ionic liquid, the liquid was removed and the ionogel was dried and weighed again. The mass of the ionogel 40/60 Syloid 72FP/EMIM Ac decreased from 0.0884 g to 0.0728 g. Thus, it can be concluded that the liquid on the surface was a mixture of water and EMIM Ac.

3.2. Hydrothermal stability

An essential feature for AD is the stability of the material in use after cycles of high/low RH being applied. Therefore, the ionogels 50/50 of Syloid AL-1FP/ EMIM Ac and 40/60 Syloid 72FP/EMIM Ac were exposed to 80% RH for 5 h, and then dried for 1 h at 80°C. As shown in Table 5, the ionogels 50/50 of Syloid AL-1FP/ EMIM Ac fragmented, losing stability, while the ionogel 40/60 Syloid 72FP/EMIM Ac remained intact although still leaking.

Table 5. Ionogel stability toward water and IL confinement stability at 80% RH.

Formulation	Initial photo	Exposed in 80% RH air for 5 h	Drying for 1 h at 80°C
50 wt.% Syloid AL-1FP, 50 wt.% EMIM Ac		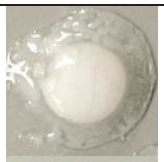	
40 wt.% Syloid 72FP, 60 wt.% EMIM Ac			

One way to solve the leakage issue involves removing the leaked liquid and repeating the hydration/dehydration cycles until leakage disappears (aging process). Therefore, the ionogel 40/60 Syloid 72FP/EMIM Ac was exposed to an 80% RH environment to adsorb water vapor for 5 h, and then the leaked liquid was removed and the ionogel was dried in oven for 1 h at 80°C. This process was repeated until no leakage occurred, after two cycles (Figure 4). The

proportion of water first increased and then remained steady at a certain value with increasing adsorption time for every cycle, and the final proportion of water decreased from 76.58 wt.% to 61.79 wt.% between cycle 1 and cycle 3. The sharp decrease in water uptake between different cycles further demonstrated that the leaked liquid around ionogels was partly IL. Indeed, the amount of IL decreased by 11.4% and only 48.60 wt.% of EMIM Ac was retained in the ionogel after 3 cycles (Figure 5) and, as shown in Figure 5, the ionogel remained intact and stable after 3 cycles. Therefore, the 50/50 Syloid 72FP/EMIM Ac composite was hydrothermally stable.

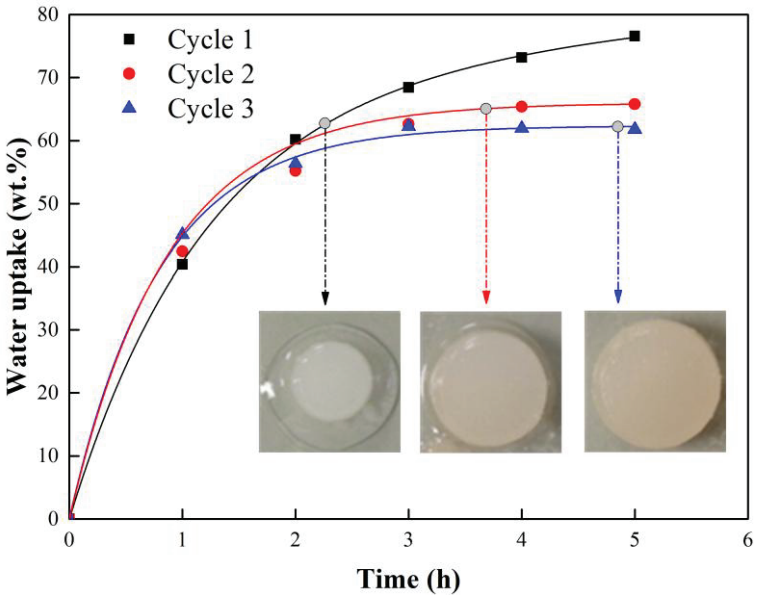

Figure 4. Adsorption capacity of aged ionogel 40/60 Syloid 72FP/EMIM Ac at 80% RH.

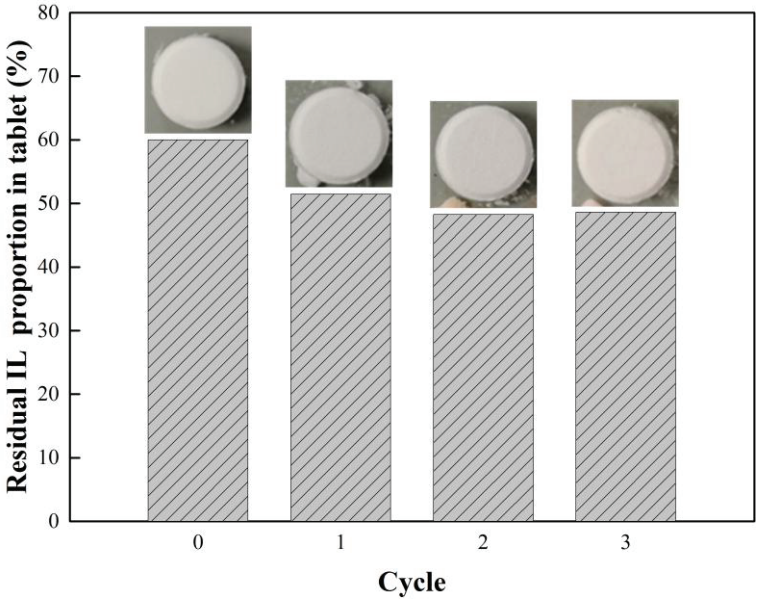

Figure 5. Residual proportion of IL of aged ionogel 40/60 Syloid 72FP/EMIM Ac at 80% RH.

A second way to solve the leakage issue is to decrease the proportion of IL in the ionogel from the beginning, but higher silica contents can lead to brittle ionogels. To resolve this issue, a small amount of water was added to ionogel to bind it before drying it. Based on cycle tests, it was concluded that the ionogel 50/50 Syloid 72FP/EMIM Ac did not leak. Thus, an ionogel with this formulation was tested for the confinement stability and stability toward water vapor adsorption. As shown in Figure 6, no leakage or fragmentation was observed after exposing the ionogel to 80% RH for 6 h and drying for 1 h at 80°C. The color of the ionogel changed over the cycles from white to transparent and returned to the original white after drying for 1 h. The water uptake increased and then leveled at 60.03% while the sorption rate showed the opposite trend. To examine the reversibility of the hydration process, the behavior of the ionogels subjected to a range of dehydrating conditions was observed. The ionogel 50/50 Syloid 72FP/EMIM Ac was tested for 3 cycles, as shown in Table 6. During every cycle, the ionogel was placed in 60% RH air for 12 h to adsorb moisture and then dried in oven at 80°C for 2 h. During drying, the ionogel changed from transparent white to opaque white. In addition, the ionogel remained intact during the entire process. The temperature swing did not affect its appearance and integrality. This demonstrates that the ionogel 50/50 Syloid 72FP/EMIM Ac shows good thermal stability at 60% RH.

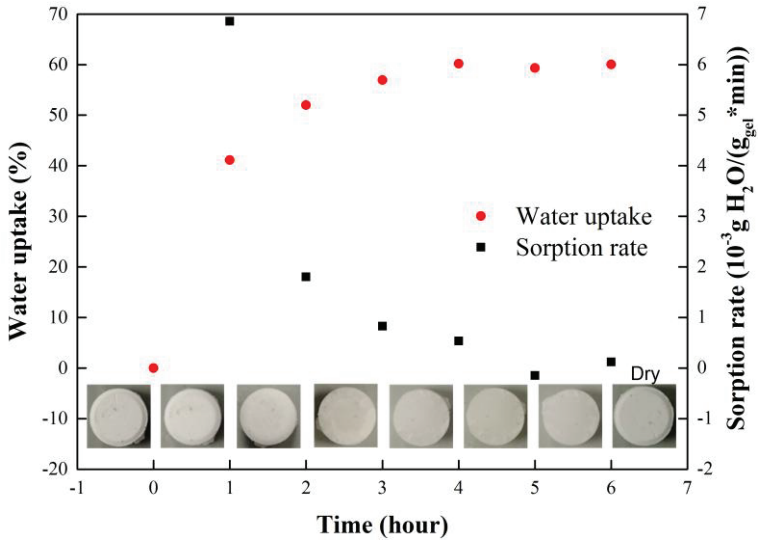

Figure 6. Adsorption performance of ionogel 50/50 Syloid 72FP/EMIM Ac at 60% RH.

Table 6. Thermal stability test results for ionogel 50/50 Syloid 72FP/EMIM Ac at 60% RH.

Cycle	0	1	2	3
Adsorption			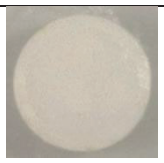	

Desorption	

Next, the two ionogels were exposed to high-RH environments to check their stability. As shown in Figure 7, 50/50 Syloid 72FP/EMIM Ac was found to be stable when exposed to high-RH air. The ionogel remained intact and no leakage occurred. As for the reversibility of the adsorption and desorption process, the water uptakes observed for the three cycles were very close, and when the hydrated ionogels were removed from the presence of water vapor and left in an oven at 80 °C, the ionogel underwent fast dehydration. The adsorption reached an equilibrium after 5 h. The sorption rate decreased gradually with increasing adsorption time. The water uptake during the first hour was almost half of the total water uptake. These results are consistent with other studies demonstrating that the solid ionogel retains the thermal properties of the IL upon confinement [40, 58]. The results also suggest that Syloid 72FP exhibits adequate gelling properties, reduces the friability of the samples, and improves their hardness and structural stability. A compliant ionogel can be obtained by pressing it with EMIM Ac and Syloid 72FP. Thus, 50/50 Syloid 72FP/EMIM Ac, which exhibited good hydrothermal stability at high RH, can be used as an adsorbent in AD.

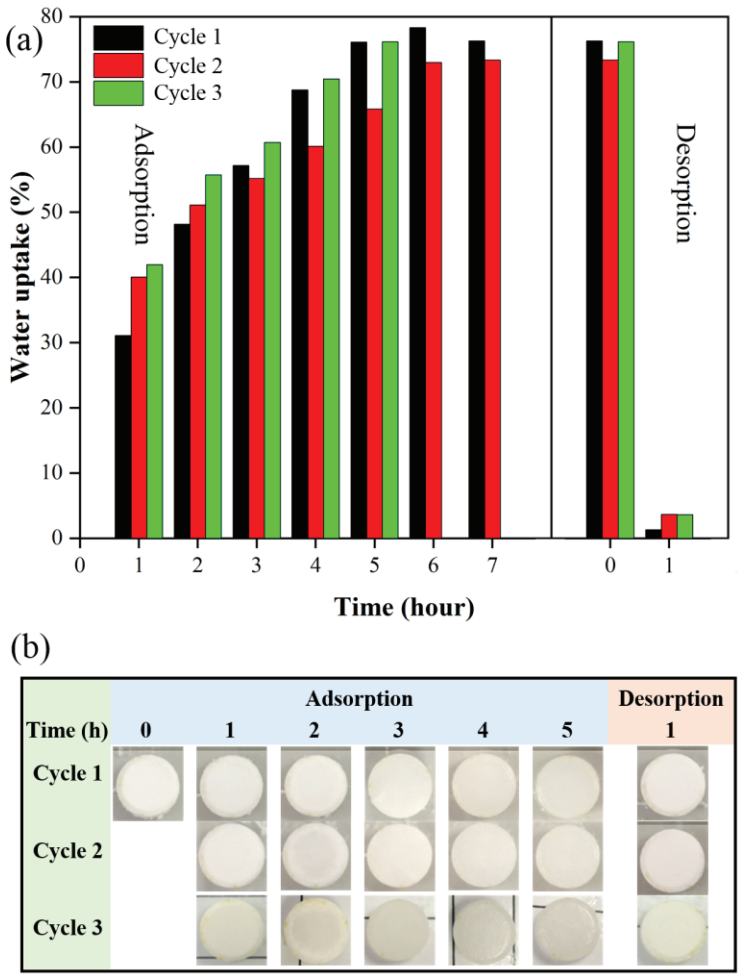

Figure 7. Hydrothermal stability and sorption properties of 50/50 Syloid 72FP/EMIM Ac at 80% RH.

3.3. Adsorption capacity

Adsorption capacity is the most important thermodynamic property in AD [56, 59]. The average sorption rates throughout the aging process of the ionogel 40/60 Syloid 72FP/EMIM Ac were calculated to illustrate the influence of the amount of IL and aging process on the sorption rate. The calculations were based on mass change of ionogel during every interval. Figure 5 shows that the proportions of EMIM Ac in the ionogel were 60 wt.% for cycle 1, 51.43 wt.% for cycle 2, and 48.23 wt.% for cycle 3. Figure 8 shows that the sorption rate degraded in the order cycle 3 > cycle 2 > cycle 1 in the first hour. However, the sorption rate increased in the order cycle 3 < cycle 2 < cycle 1 in the following four hours. Syloid 72FP showed a highly developed network of mesopores that provided access to a large surface area. When the ionogel formed, the IL filled most of the pores. However, it was crucial to maintain a certain porosity, which helped water vapor transfer into the ionogel. In the ionogel with less IL water vapor can diffuse into IL very fast. A comparison between the adsorption behaviors of aged ionogels 40/60 Syloid 72FP/EMIM Ac (Figure 8) and 50/50 Syloid 72FP/EMIM Ac (Figure 6) showed that they exhibited almost the same water uptake (about 60.00%) after attaining adsorption equilibrium. In the first hour, the sorption rates showed obvious differences: this is because aged ionogel 5 had a higher porosity due to IL loss owing to water vapor dispersion into the IL.

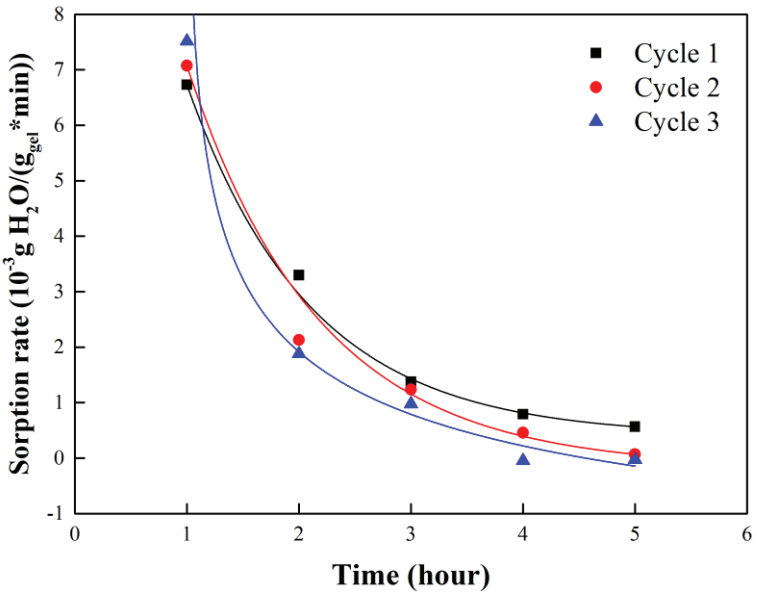

Figure 8. Sorption rate of ionogel 40/60 Syloid 72FP/EMIM Ac and aging process.

The adsorption isotherms of EMIM Ac, the ionogel 50/50 Syloid 72FP/EMIM Ac, silica gel, and activated carbon [60] at 25°C are outlined in Figure 9. The adsorption isotherms of EMIM Ac and the ionogel were type III with a characteristic linear uptake at low vapor concentrations (below 50% RH) and a strong increase in adsorption at higher vapor

concentrations (above 50% RH). At a lower RH, the hydroxyl group of water preferentially interacted with the carbonyl group of the anionic part of EMIM Ac [61]. These adsorbed water vapor molecules then acted as secondary sites for further water adsorption, and hydrogen bonds between water vapor molecules formed at a higher RH. This type of isotherm was observed because the water vapor interacted with the ionogel in an energetically comparable manner (i.e., showing a heat of sorption similar to the heat of condensation). This caused only very few molecules to adsorb at a low RH (they prefer to interact loosely in the vapor phase) followed by condensation at a higher RH on the few initially adsorbed molecules. Such an effect can be described as cluster formation since there is no monolayer formation occurred. Because of this property, water vapor easily desorbed from the ionogel, indicating a low regeneration temperature and fast desorption in the AD system. As for the adsorption capacity, the water uptake of the ionogel was 1.64 g_{water} $g_{ionogel}^{-1}$ while the water uptake of EMIM Ac was 1.98 g_{water} g_{IL}^{-1} at 90% RH. Because the water uptake of silica nanoparticles is far less than that of EMIM Ac, EMIM Ac in the ionogel contributes to the majority of the water uptake. In addition, only 50 wt.% EMIM Ac was confined in the ionogel, and the adsorption capacity of the ionogel was lower than that of pure EMIM Ac. This suggests that the adsorption capacity is controlled by the amount of IL in the ionogel. Compared with that of Syloid 72FP silica and activated carbon, the water uptake of the ionogel was ~3 and ~4 times at 90% RH, respectively.

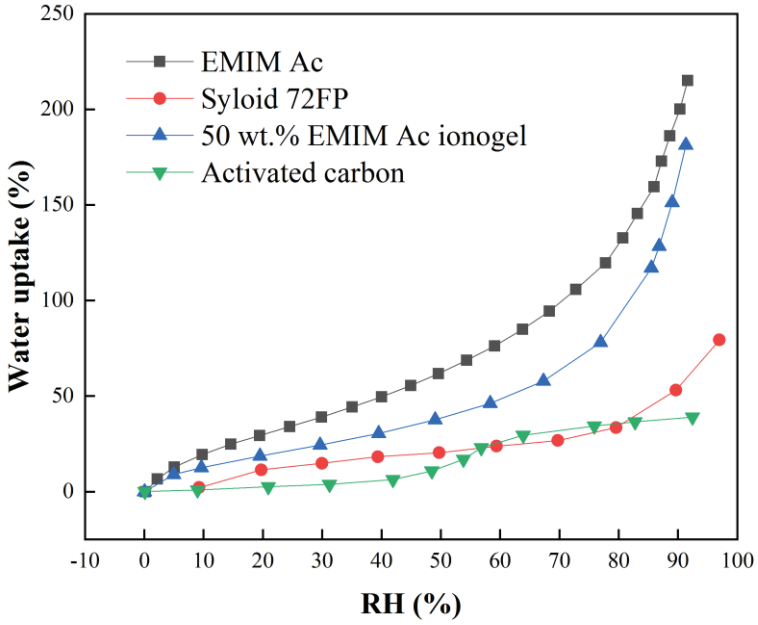

Figure 9. Adsorption isotherms of EMIM Ac, 50 wt.% EMIM Ac ionogel, Syloid 72FP, and activated carbon at 25 °C.

4. Conclusion

In this study, we analyzed the influence of formulation and preparation of silica nanoparticle-based ionogels on their features such as their confinement stability, thermal stability, water stability, and adsorption capacity. Four conclusions could be obtained: 1) incipient wetness impregnation can be used to prepare silica/IL composite ionogel; 2) a

composition of 50 wt.% EMIM Ac and 50 wt.% Syloid 72FP was the most suitable formulation for obtaining a well-confined and hydrothermally stable ionogel; 3) the sorption rate and adsorption capacity increased with increase in the RH; 4) water uptake of the synthesized ionogel was ~3 times of that of Syloid 72FP silica and ~4 times of that of activated carbon at 90% RH. These results suggest that the prepared ionogel shows great potential for adsorption desalination.

Conflicts of interest

There are no conflicts of interest to declare.

Acknowledgements

Funding: This work was supported by the EPSRC within framework of the project "Micro-scale energy storage for super-efficient wet appliances" (EP/P010954/1).

References

[1] He Z, Zhao Z, Zhang X, Feng H. Thermodynamic properties of new heat pump working pairs: 1, 3-Dimethylimidazolium dimethylphosphate and water, ethanol and methanol. Fluid Phase Equilibria. 2010;298(1):83-91.

[2] Cao Y, Mu T. Comprehensive investigation on the thermal stability of 66 ionic liquids by thermogravimetric analysis. Industrial & engineering chemistry research. 2014;53(20):8651-64.

[3] Freire MG, Santos LM, Fernandes AM, Coutinho JA, Marrucho IM. An overview of the mutual solubilities of water–imidazolium-based ionic liquids systems. Fluid Phase Equilibria. 2007;261(1):449-54.

[4] Fehrmann R, Riisager A, Haumann M. Supported Ionic Liquids: Fundamentals and Applications2014.

[5] Zhao H, Xia S, Ma P. Use of ionic liquids as 'green' solvents for extractions. Journal of Chemical Technology & Biotechnology. 2010;80(10):1089-96.

[6] Wu F, Zhu N, Bai Y, Liu L, Zhou H, Wu C. Highly safe ionic liquid electrolytes for sodium-ion battery: wide electrochemical window and good thermal stability. ACS applied materials & interfaces. 2016;8(33):21381-6.

[7] Wadekar VV. Ionic liquids as heat transfer fluids–an assessment using industrial exchanger geometries. Applied Thermal Engineering. 2017;111:1581-7.

[8] Morandeira L, Álvarez MaS, Markiewicz M, Stolte S, Rodríguez A, Sanromán MAn, et al. Testing true choline ionic liquid biocompatibility from a biotechnological standpoint. ACS Sustainable Chemistry & Engineering. 2017;5(9):8302-9.

[9] Bates ED, Mayton RD, Ntai I, Davis JJH. CO2 capture by a Task-Specific Ionic Liquid. Journal of the American Chemical Society. 2002;124(6):926-7.

[10] Heym F, Haber J, Korth W, Etzold BJ, Jess A. Vapor Pressure of Water in Mixtures with Hydrophilic Ionic Liquids–A Contribution to the Design of Processes for Drying of Gases by Absorption in Ionic Liquids. Chemical Engineering & Technology. 2010;33(10):1625-34.

[11] Aken KL, Van, Majid B, Yury G. Formulation of ionic-liquid electrolyte to expand the voltage window of supercapacitors. Angewandte Chemie. 2015;54(16):4806-9.

[12] Askalany AA, Freni A, Santori G. Supported ionic liquid water sorbent for high throughput desalination and drying. Desalination. 2019;452:258-64.

[13] Dong H, Zhang L, Ling Z, Zhao J, Song Y. The Controlling Factors and Ion Exclusion Mechanism of Hydrate-Based Pollutant Removal. ACS Sustainable Chemistry & Engineering. 2019;7(8):7932-40.

[14] Song Y, Dong H, Yang L, Yang M, Li Y, Ling Z, et al. Hydrate-based heavy metal separation from aqueous

solution. Scientific Reports. 2016;6:21389.
[15] Chakraborty A, Thu K, Saha BB, Ng KC. Adsorption- Desalination Cycle: John Wiley & Sons, Inc., 2012.
[16] Wang X, Ng KC. Experimental investigation of an adsorption desalination plant using low-temperature waste heat. Applied Thermal Engineering. 2005;25(17-18):2780-9.
[17] Wu JW, Hu EJ, Biggs MJ. Thermodynamic cycles of adsorption desalination system. Applied energy. 2012;90(1):316-22.
[18] Olkis C, Brandani S, Santori G. A small-scale adsorption desalinator. Energy Procedia. 2019;158:1425-30.
[19] Thu K, Saha BB, Chakraborty A, Chun WG, Ng KC. Study on an advanced adsorption desalination cycle with evaporator–condenser heat recovery circuit. International Journal of heat and mass transfer. 2011;54(1-3):43-51.
[20] Ng K, Chua H, Chung C, Loke C, Kashiwagi T, Akisawa A, et al. Experimental investigation of the silica gel–water adsorption isotherm characteristics. Applied Thermal Engineering. 2001;21(16):1631-42.
[21] Thu K, Chakraborty A, Saha BB, Ng KC. Thermo-physical properties of silica gel for adsorption desalination cycle. Applied Thermal Engineering. 2013;50(2):1596-602.
[22] Ng KC, Thu K, Kim Y, Chakraborty A, Amy G. Adsorption desalination: An emerging low-cost thermal desalination method. Desalination. 2013;308(Supplement C):161-79.
[23] Olkis C, Brandani S, Santori G. Design and experimental study of a small scale adsorption desalinator. Applied Energy. 2019;253:113584.
[24] Olkis C, Brandani S, Santori G. Cycle and performance analysis of a small-scale adsorption heat transformer for desalination and cooling applications. Chemical Engineering Journal. 2019;378:122104.
[25] Kim Y-D, Thu K, Ng KC. Adsorption characteristics of water vapor on ferroaluminophosphate for desalination cycle. Desalination. 2014;344:350-6.
[26] Santori G, Di Santis C. Optimal fluids for adsorptive cooling and heating. Sustainable Materials and Technologies. 2017;12:52-61.
[27] Zejli D, Benchrifa R, Bennouna A, Bouhelal O. A solar adsorption desalination device: first simulation results. Desalination. 2004;168:127-35.
[28] Youssef PG, Mahmoud SM, Al-Dadah RK. Performance analysis of four bed adsorption water desalination/refrigeration system, comparison of AQSOA-Z02 to silica-gel. Desalination. 2015;375:100-7.
[29] Youssef P, Al-Dadah R, Mahmoud S, Dakkama H, Elsayed A. Effect of evaporator and condenser temperatures on the performance of adsorption desalination cooling cycle. Energy Procedia. 2015;75:1464-9.
[30] Youssef PG, Mahmoud SM, Al-Dadah RK. Numerical simulation of combined adsorption desalination and cooling cycles with integrated evaporator/condenser. Desalination. 2016;392:14-24.
[31] Thu K, Chakraborty A, Kim Y-D, Myat A, Saha BB, Ng KC. Numerical simulation and performance investigation of an advanced adsorption desalination cycle. Desalination. 2013;308:209-18.
[32] Chakraborty A, Thu K, Saha BB, Ng KC. Adsorption- Desalination Cycle. Advances in Water Desalination. 2012:377-451.
[33] Wu JW, Hu EJ, Biggs MJ. Thermodynamic analysis of an adsorption-based desalination cycle (part II): effect of evaporator temperature on performance. Chemical Engineering Research and Design. 2011;89(10):2168-75.
[34] Arellano IHJ, Guarino JG, Paredes FU, Arco SD. Thermal stability and moisture uptake of 1-alkyl-3-methylimidazolium bromide. Journal of thermal analysis and calorimetry. 2011;103(2):725-30.
[35] Di Francesco F, Calisi N, Creatini M, Melai B, Salvo P, Chiappe C. Water sorption by anhydrous ionic liquids. Green Chemistry. 2011;13(7):1712-7.
[36] Cao Y, Chen Y, Sun X, Zhang Z, Mu T. Water sorption in ionic liquids: kinetics, mechanisms and

hydrophilicity. Physical Chemistry Chemical Physics. 2012;14(35):12252-62.
[37] Makino T. In situ Raman study of dissolved carbon-dioxide induced changes of imidazolium-based ionic liquids. Journal of Physics Conference. 2010;215:012068.
[38] Xie Z-L, Jeličić A, Wang F-P, Rabu P, Friedrich A, Beuermann S, et al. Transparent, flexible, and paramagnetic ionogels based on PMMA and the iron-based ionic liquid 1-butyl-3-methylimidazolium tetrachloroferrate (III)[Bmim][FeCl4]. Journal of Materials Chemistry. 2010;20(42):9543-9.
[39] Garaga MN, Persson M, Yaghini N, Martinelli A. Local coordination and dynamics of a protic ammonium based ionic liquid immobilized in nano-porous silica micro-particles probed by Raman and NMR spectroscopy. Soft Matter. 2016;12(9):2583-92.
[40] Vioux A, Viau L, Volland S, Le Bideau J. Use of ionic liquids in sol-gel; ionogels and applications. Comptes Rendus Chimie. 2010;13(1):242-55.
[41] Susan H, Kaneko T, Noda A, Watanabe M. Ion gels prepared by in situ radical polymerization of vinyl monomers in an ionic liquid and their characterization as polymer electrolytes. Journal of the American Chemical Society. 2005;127(13):4976-83.
[42] Le Bideau J, Viau L, Vioux A. Ionogels, ionic liquid based hybrid materials. Chemical Society Reviews. 2011;40(2):907-25.
[43] Scott MP, Rahman M, Brazel CS. Application of ionic liquids as low-volatility plasticizers for PMMA. European Polymer Journal. 2003;39(10):1947-53.
[44] Garaga MN, Aguilera L, Yaghini N, Matic A, Persson M, Martinelli A. Achieving enhanced ionic mobility in nanoporous silica by controlled surface interactions. Physical Chemistry Chemical Physics. 2017;19(8):5727-36.
[45] Li D, Shi F, Guo S, Deng Y. One-pot synthesis of silica gel confined functional ionic liquids: effective catalysts for deoximation under mild conditions. Tetrahedron letters. 2004;45(2):265-8.
[46] Ueno K, Hata K, Katakabe T, Kondoh M, Watanabe M. Nanocomposite ion gels based on silica nanoparticles and an ionic liquid: ionic transport, viscoelastic properties, and microstructure. The Journal of Physical Chemistry B. 2008;112(30):9013-9.
[47] Negre L, Daffos B, Taberna P-L, Simon P. Silica-Based Ionogel Electrolyte for Electrical Double Layer Capacitors. Conference Silica-Based Ionogel Electrolyte for Electrical Double Layer Capacitors. The Electrochemical Society, p. 952-.
[48] Römich C, Merkel NC, Valbonesi A, Schaber K, Sauer S, Schubert TJS. Thermodynamic Properties of Binary Mixtures of Water and Room-Temperature Ionic Liquids: Vapor Pressures, Heat Capacities, Densities, and Viscosities of Water + 1-Ethyl-3-methylimidazolium Acetate and Water + Diethylmethylammonium Methane Sulfonate. Journal of Chemical & Engineering Data. 2012;57(8):2258–64.
[49] Katayanagi H, Nishikawa K, Shimozaki H, Miki K, Westh P, Koga Y. Mixing Schemes in Ionic Liquid−H 2 O Systems: A Thermodynamic Study. Jphyschemb. 2004;108(50):19451-7.
[50] Zhang L, Han J, Wang R, Qiu X, Ji J. Isobaric Vapor−Liquid Equilibria for Three Ternary Systems: Water + 2Propanol + 1Ethyl3-methylimidazolium Tetrafluoroborate, Water + 1Propanol + 1Ethyl3-methylimidazolium Tetrafluoroborate, and Water + 1Propanol + 1Butyl3-methylimidazolium Tetrafluorobor. Journal of Chemical & Engineering Data. 2007;52(4):1401-7.
[51] Doker M, Gmehling J. Measurement and prediction of vapor–liquid equilibria of ternary systems containing ionic liquids. Fluid Phase Equilibria. 2005;227(2):255-66.
[52] Simoni LD, Ficke LE, Lambert CA, Stadtherr MA, Brennecke JF. Measurement and Prediction of Vapor−Liquid Equilibrium of Aqueous 1Ethyl3-methylimidazolium-Based Ionic Liquid Systems. Indengchemres. 2010;49(8):3893-901.

[53] Zhang F, Zheng F, Wu X, Yang X, Zhang Q, Yin Y. Thermophysical properties of [EMIm] Ac and its binary and ternary mixtures with water and graphene nanoplatelets for absorption refrigeration. AIP Advances. 2019;9(5):055124.

[54] Hu C, Jiang S, Wu Z, Miao M. Influence of ionic liquids on the species and content of coal functional group. Electron J Geotech Eng. 2014;19:1365-75.

[55] Miyauchi M, Miao J, Simmons TJ, Lee J-W, Doherty TV, Dordick JS, et al. Conductive cable fibers with insulating surface prepared by coaxial electrospinning of multiwalled nanotubes and cellulose. Biomacromolecules. 2010;11(9):2440-5.

[56] Aristov Y. Concept of adsorbent optimal for adsorptive cooling/heating. Applied Thermal Engineering. 2014;72(2):166-75.

[57] Žumár J, Pavlík Z. Adsorption of Water Vapor in Selected Sandstone Influenced by Different Method of Measurement Using Dynamic Vapor Sorption Device. Advanced Materials Research. 2014;982:16-21.

[58] Cerclier CV, Zanotti J-M, Le Bideau J. Ionogel based on biopolymer–silica interpenetrated networks: dynamics of confined ionic liquid with lithium salt. Physical Chemistry Chemical Physics. 2015;17(44):29707-13.

[59] Shahzad MW, Ng KC, Thu K, Saha BB, Chun WG. Multi effect desalination and adsorption desalination (MEDAD): A hybrid desalination method. Applied Thermal Engineering. 2014;72(2):289-97.

[60] Shaoying Q, K James H, Rood MJ, Cal MP. Equilibrium and heat of adsorption for water vapor on activated carbon. Journal of Environmental Engineering. 2000;126(3):267-71.

[61] Ghazvini MS, Pulletikurthi G, Tong C, Kuhl C, Endres F. Electrodeposition of Zinc from 1-ethyl-3-methylimidazolium acetate-water Mixtures: Investigations on the Applicability of the Electrolyte for Zn-Air Batteries. Journal of The Electrochemical Society. 2018;165(9):D354-D63.